Hydrodynamic Similarity of Solids Motion and Mixing in Bubbling Fluidized Beds

John Sanderson and Martin Rhodes
Dept. of Chemical Engineering, Monash University, P. O. Box 36, Clayton, Victoria, 3800, Australia

Solids motion and solids mixing behavior are important in many fluidized-bed applications, and yet, in the evaluation of hydrodynamic similarity criteria, relatively few studies have considered these phenomena directly. This work reports on a series of physical experiments involving solids motion and solids mixing undertaken in a number of freely bubbling fluidized beds scaled using the "simplified" scaling criteria. In the first set of experiments, the motion of large neutrally buoyant particles in bubbling beds of a finer material was compared using a simple float-tracer experiment in beds that were 300 mm, 600 mm, and 1,560 mm in dia. The distribution of circulation times for the float-tracers was found to scale well across the majority of gas velocities considered when the scaling law was followed, but discrepancies were noted when either the bulk bed material or large tracer particle sizes were mismatched. These results demonstrate that the circulation of large neutrally buoyant particles within the correctly scaled bubbling beds is indeed a "scaleable" phenomenon across a wide range of bed sizes, and this has useful consequences for fluidized-bed applications involving floating bodies. In the second set of experiments, solids downflow velocities were compared in scaled beds that were 146 mm and 300 mm in dia. using a novel application of electrical–capacitance tomography (ECT). The measured solids downflow velocities showed qualitative agreement with the scaling law and correlations in the literature. The novel tracer technique was only moderately successful in this application, but is worthy of further investigation, as the approach may serve to enhance the capabilities of existing ECT equipment.

Introduction

The extent of solids mixing in bubbling fluidized beds is an important factor in their design for many applications. Mixing affects heat transfer, mass transfer, and can significantly influence the overall reaction rate in a fluidized-bed reactor. In bubbling fluidized-bed coal combustors, the motion of the larger and lighter coal particles within the bulk bed material will have consequences for the combustion behavior (Agarwal and LaNauze (1989); Prins et al. (1989); Hesketh and Davidson (1991)). Therefore, the effect of a change in bed size on the motion of bed materials and large particles is an important scale-up consideration in the many processes where these phenomena play a role.

Historically, the effect of a scale change on bubbling-bed behavior has received much attention over the years, and in the early 1980s hydrodynamic similarity criteria were recognized as a possible way of predicting the physical behavior of a large bubbling fluidized bed based on measurements made in a small one. These so-called scaling laws took the form of a set of dimensionless groups which, if maintained constant in two different-sized bubbling beds, should ensure that the physical phenomena occurring in the beds was scaled with their size.

Fitzgerald and Crane (1980) were one of the first to suggest and experimentally test this approach, which was further evaluated in a subsequent study (Fitzgerald et al., 1984). Glicksman et al. (1984) also proposed a similar set of dimensionless groups, but his approach allowed the cases of inertial-dominated and viscous-dominated flow to be considered separately, resulting in simplifications to the set of dimensionless groups under those conditions. Horio et al. (1986a) suggested an alternative form of scaling relationship ex-

Correspondence concerning this article should be addressed to M. J. Rhodes.

pressed as a pair of equations. This was later shown (Glicksman, 1988) to be equivalent to the viscous-dominated version of Glicksman's scaling relationships. The importance of the solid-to-gas density ratio was pointed out by Glicksman et al. (1993). Farrel et al. (1998) experimentally demonstrated the failure of the viscous-dominated scaling law under conditions in which the solid-to-gas density ratio was mismatched and the particle Reynolds number exceeded $Re_p = 4$ (the accepted limit for the viscous-dominated regime).

It is perhaps appropriate at this point to clarify what is generally meant by the term "simplified scaling law" as it relates to the inclusion of the solid-to-gas density-ratio parameter. The literature is somewhat confusing, because the scaling relationship of Horio et al. (1986a) does not explicitly require the solid-to-gas density ratio to be matched between the two scaled systems, yet it has often been experimentally evaluated in systems using the same solids type and fluidizing gas, thus maintaining a constant solid-to-gas density ratio inadvertently. So, in fact, the term "simplified scaling law" most commonly refers to the Horio scaling criteria plus the additional requirement of matching the solid-to-gas density ratio, or expressed in another way: the viscous-dominated version of the Glicksman groups plus the solid-to-gas density ratio (which is the form specifically developed and referred to as the simplified scaling law in Glicksman et al. (1993)). In summary (and omitting for the moment the additional particle-related requirements of similar size distribution and sphericity) the simplified scaling law for bubbling fluidization can be expressed

- Based on the form of Horio et al. (1986a), as

$$\left.\begin{aligned} &U_2 - U_{mf2} = \sqrt{m}\,(U_1 - U_{mf1}) \\ &U_{mf2} = \sqrt{m}\,U_{mf1} \\ &\text{similar bed geometry} \\ &\frac{\rho_{s1}}{\rho_{f1}} = \frac{\rho_{s2}}{\rho_{f2}} \end{aligned}\right\} \qquad (1)$$

where this last requirement has often been satisfied inadvertently by having systems where $\rho_{s2} = \rho_{s1}$ and $\rho_{f2} = \rho_{f1}$ by using the same gas and solid material at both scales.

- As suggested by Glicksman et al. (1993) (for bubbling fluidization)

$$\frac{U^2}{gL}, \quad \frac{U}{U_{mf}}, \quad \frac{L_1}{L_2}, \quad \frac{\rho_s}{\rho_f} \qquad (2)$$

Both Eqs. 1 and 2 are equivalent, from a simple extension of the equivalency demonstrated by Glicksman (1988). Note that in this work we will consider the simplified scaling law in the form in which it is expressed in Eq. 1.

Now, before such scaling criteria can be applied with confidence in a "real" situation, experimental verification is required in order to check that fluidized systems operated in accordance with the proposed criteria do in fact exhibit scaled behavior. To this end, the proposed bubbling-bed scaling laws in their various forms were experimentally verified in a number of different scale change scenarios by their proponents and other workers, with some encouraging results. Generally, the verification has involved comparisons of bubble-related measurements such as pressure fluctuations (Nicastro and Glicksman, 1984; Roy and Davidson, 1989; Leu and Lan, 1992), visual bubble analysis (Fitzgerald and Crane, 1980; Horio et al., 1986a; Newby and Keairns, 1986) and local voidage fluctuations (Almstedt and Zakkay, 1990). In a practical sense, bubble-related measurements are often easier to carry out and compare quantitatively, but the question arises as to whether similarity in these measurements really demonstrates similarity in solids mixing. For this to be the case, the assumption must be made that solids mixing phenomena are completely controlled by bubble behavior in the bed, and all the bubble characteristics (including wake and drift fractions) have scaled correctly. While this assumption may indeed be valid, direct examination of the motion of solids in systems scaled using similarity criteria is necessary to confirm it. However, to date, no verification of the full set of scaling laws appears to have been carried out using solids mixing techniques, and we could only identify two studies that considered the motion of solids in relation to scale change with the simplified scaling laws. These studies are considered below.

In their original development, Horio et al. (1986a) showed that their scaling law was in agreement with some models for radial and axial solids dispersion. Subsequently, Horio et al. (1986b) tested the application of the simplified scaling law to solids mixing behavior. They measured the radial dispersion of tracer solids and radial and axial dispersion of large, neutrally buoyant particles in beds from 50-mm to 600-mm dia. using a transient response/bed sectioning technique. The agreement of the results was encouraging, and this study also represents the largest bed size in which similarity of solids mixing has been considered so far. However, their experimental comparison suffers from the shortcoming that no deliberate mismatch experiment was performed. So there is no way to be sure that agreement of the results confirms the success of the scaling criteria, or whether the particular measurements being compared would have been generally similar in bubbling fluidized beds anyway.

In a more recent study, Stein et al. (1998) used positron emission particle tracking (PEPT) to follow the motion of a single tagged bed particle in several air-fluidized bubbling beds (70-mm to 240-mm dia.) that appear to have been scaled using the viscous-limit scaling parameters in one comparison and the simplified scaling parameters in another. A comparison of solids circulation frequency produced reasonably similar results in the cases presented, and compared favorably with the inverse of bed turnover time as estimated using the correlations of Kunii and Levenspiel (1969) and Baeyens and Geldart (1986). Similarity broke down for the smallest column, which was found to be slugging. Again, no deliberate mismatch was reported on, and the agreement of the systems in which the density ratio was not matched is cause for concern, as it appears to be in contradiction with the recommendations of Glicksman et al. (1993) and Farrel et al. (1998), since the systems were operated at particle Reynolds numbers well beyond that of the viscous regime (that is, $Re_p \geq 4$).

Given that the success of the simplified scaling law with respect to solids motion is still somewhat speculative, the present investigation was undertaken in order to test the sim-

plified scaling laws over a larger scale change than had been done previously, and explore deliberately mismatched scenarios to confirm that agreement of our measurements was indeed a direct result of matching the similarity criteria. It was also an opportunity to trial the existing electrical–capacitance tomography (ECT) system for solids motion studies and to augment pressure fluctuation comparisons carried out previously on the same bubbling-bed equipment (Sanderson et al., 2001).

In this work, the solids motion comparisons take the form of circulation time distributions for neutrally buoyant large particles in the 300-mm, 600-mm, and 1,560-mm beds, and solids downflow velocities for the bulk bed material in the 146-mm and 300-mm beds. All beds were geometrically similar cold models and employed scaled bubble-cap distributors.

Similarity in the Motion of Large Neutrally Buoyant Particles

Background

Apart from the study of Horio et al. (1986b), the motion of larger and lighter particles has not been considered with regard to hydrodynamic similarity criteria. Horio et al. presented an equation of motion for a floating body in order to demonstrate the theoretical possibility of the dimensionless object motion being identical in scaled fluidized beds, and we will now consider some observations of large-particle behavior from other studies for possible consistency with the simplified scaling laws.

It has been observed that objects with a density near that of the bulk emulsion at minimum fluidization conditions circulate throughout the whole of a bubbling bed (for example, Nguyen and Grace, 1978), although flat objects have a greater tendency to settle to the distributor, particularly at low gas velocities (Nienow et al., 1978). For large objects with a density that promotes their circulation throughout the bed, the object is carried upwards to the bed surface in an irregular fashion under the influence of rising bubbles, and moves downwards under the influence of the dense phase (Nienow et al., 1978; Lim and Agarwal, 1994). Because they are affected by bubble and solids behavior, the motion of these large, neutrally buoyant objects has been used in hydrodynamic studies. For example, Merry and Davidson (1973) used a large "radio-pill" as a tracer in an experimental investigation of gulf-streaming; and Bellgardt and Werther (1986) used subliming dry-ice pellets to study solids mixing.

Lim and Agarwal (1994) studied the motion of large, neutrally buoyant objects in a two-dimensional bed, relating the upwards and downwards velocities of the object to the average measured bubble rise velocity (U_B) and the solids downflow velocity (U_{sd}). They observed that the objects moved upwards under the influence of rising bubbles, and did so in a hesitating fashion, prompting them to characterize the upwards motion with two measures of upwards velocity. The average rise velocity of the object was found to be about $0.07U_B$, but the average upwards velocity component of the object (that is, excluding the time spent in hesitating motions) was closer to $0.3U_B$. The object descended at a velocity comparable with the solids downflow velocity (U_{sd}). These results were in good agreement with the results of the previous three-dimensional (3-D) work of Rios et al. (1986), and Nienow et al. (1978). Given the consistency of these studies, the observed relationship of Lim and Agarwal between the upwards and downwards velocities of the body compared with that of bubbles and bulk solids may hold generally for bubbling beds. If that is the case, then the upwards and downwards velocities of the large particle should scale according to the scaling laws if the bubble rise velocity and solids downflow velocities do. Hence, the motion of the large particle can be used as a test for hydrodynamic similarity.

In the present work, we compare the dimensionless circulation time distribution of large, neutrally buoyant particles in the scaled fluidized beds as a test of hydrodynamic similarity. This measurement, taken by recording the time between successive appearances of a large particle at the bed surface, is a function of the upwards and downwards velocities of the particle, and the proportion of time spent traveling in each direction. Although the large-particle velocities cannot be calculated directly from this measurement alone, we can use the circulation time distribution as a hydrodynamic indicator (rather like the way in which pressure fluctuations are often used in hydrodynamic comparisons). It is clear that if the motion of the large particle has not scaled correctly, then the distribution of resulting circulation times will not scale either.

Experimental

In this part of the investigation three air-fluidized bubbling beds of Geldart B silica sand (particle sphericity approximately 0.86) were employed. (Particle-size distributions for all bed and tracer materials have been presented in Sanderson, 2003.) They were of a cylindrical cross section, with diameters of 300 mm, 600 mm, and 1,560 mm. Bed aspect ratios were scaled, with $H_s/D \approx 0.67{:}1$. All beds employed geometrically similar bubble-cap distributors designed to provide a minimum pressure drop of at least 0.3 times the bed pressure drop at the lowest gas velocity investigated ($U/U_{mf} = 1.25$). Each distributor used 18 bubble caps in a triangular-pitch arrangement. The central location was reserved for a solids-drain port (except in the 600-mm bed where solids were drained through a side opening). Distributor details are provided in Figure 1a.

The setup for investigating the circulation time distribution for the large particles is shown in Figure 1b. Three tracers with identical diameter and density (but different color) were placed into a given bed for each experiment. For our experiments, we define the circulation time as *the time between successive appearances of a given tracer at the bed surface*. The appearance and disappearance of the float tracers at the bed surface was recorded using a video camera mounted in the freeboard region. The camera was contained in a sealed housing (of the type normally used for underwater filming) to prevent solids ingress into the mechanism. The size and density of the float tracers for the correctly scaled similarity experiments were as specified in Table 1. The tracers were made from ping-pong balls loaded with sand and polythene (1,560-mm bed) and wooden balls loaded with several grains of lead shot sealed into a diametral hole (600-mm and 300-mm beds).

The bulk densities of the bed materials shown in Table 1 were calculated based on the measured bed height for a known mass of solids in a preliminary small-scale test of each material. Because the density ratio of the large particle to

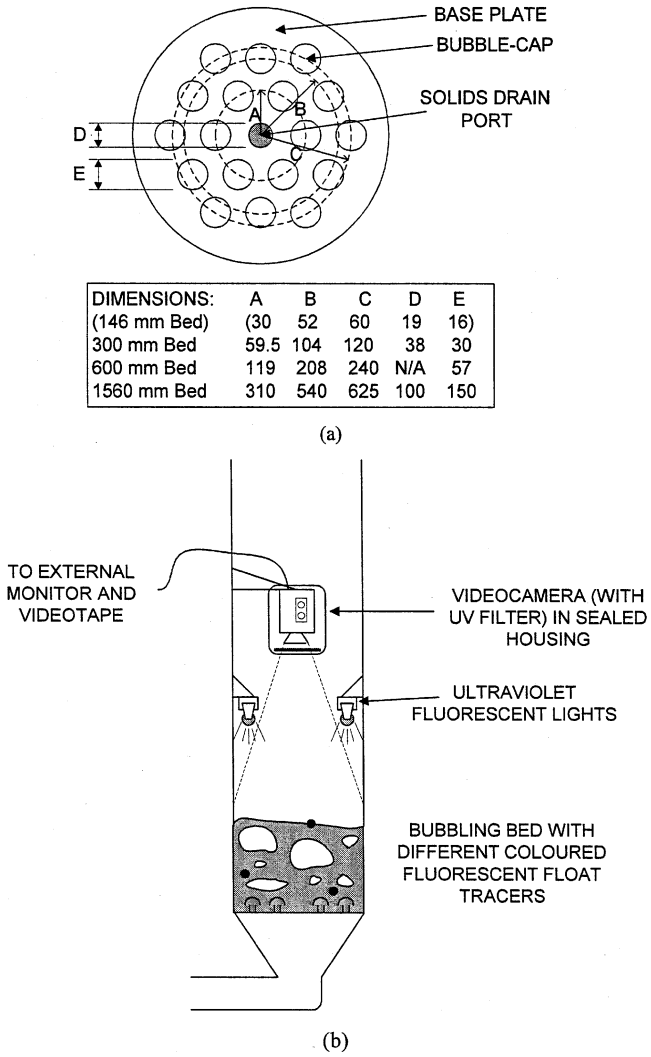

Figure 1. (a) Detail of the scaled bubble-cap distributor design employed at all bed scales (note that data for the 146-mm bed distributor (used in solids downflow velocity experiments) have also been included); (b) experimental technique for monitoring the circulation of large neutrally buoyant particles in bubbling fluidized beds of 300-mm, 600-mm, and 1,560-mm dia.

The camera was set up so that the field of view was wide enough to cover the entire bed surface when fluidized; the height of the lamps was then adjusted so that they were just clear of frame.

bulk bed material was not perfectly matched in all cases, a preliminary experiment was performed in the 1,560-mm bed with large particles of various densities. It was found that within the range considered (1,310 to 1,410 kg/m^3), the large-particle density had very little effect on the circulation time distribution. This is in agreement with other workers, for example, Merry and Davidson 1973), and demonstrates that the small density differences present in our similarity experiments can be safely ignored.

Each float tracer was painted with a different color fluorescent paint (red, green, and blue), and the bed surface was

Table 1. Float Tracer Specifications for Hydrodynamic Similarity Experiments

D (mm)	1,560	600	300
D_t (mm)	37.8	14.6	7.3
D/D_t	41.3	41.1	41.1
ρ_t (kg/m^3)	1,360	1,350	1,350
$\rho_{bed(mf)}$	1,570	1,570	1,540
$\rho_t/\rho_{bed(mf)}$	0.866	0.860	0.877

Note: D refers to bed diameter; D_t is the tracer diameter; ρ_t is the tracer density; and $\rho_{bed(mf)}$ is the estimated density of the bed materials at minimum fluidization.

illuminated with "soft" ultraviolet light from blacklight fluorescent tubes, so that each time a tracer appeared at the bed surface it could be easily and clearly distinguished in the video images. Three tracers were used to increase the number of statistics generated. The time between appearances of a given color tracer was logged from the videotape for different operating conditions using the following procedure.

The times at which a tracer appeared at the bed surface were logged in real-time during the video playback of each experiment by recording the state of three momentary push-buttons (one button for each tracer color) using a data-acquisition PC sampling at 5 Hz. (That is, as each colored tracer appeared at the bed surface, the observer momentarily pushed the appropriate button to record the appearance.) The resulting time series of square-wave pulses could then be used to determine the time spent by the tracers below the bed surface by measuring the time-differential between rising edges of each successive square wave.

Figure 2 shows the procedure graphically, from which it can be seen that the recorded time below the bed surface will approximate the actual time below the bed surface if:

(a) The time at the surface is short compared with the time below the surface, and

(b) The observer reaction times are short and/or constant.

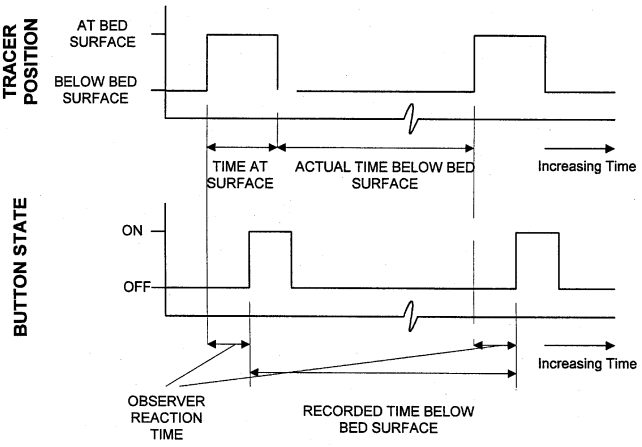

Figure 2. Graphical representation of the float-tracer logging procedure.

Upper chart refers to the actual location of the large tracer; the lower chart refers to the recorded signal from the push button. The recorded time below the bed surface will approximate the actual time below the bed surface if the observer reaction time is short and/or constant, and the time at the surface is short compared with the time below the surface.

Table 2. Operating Conditions for the Float Tracer Circulation Time Similarity Experiments

Bed Dia. D (mm)	Mean Bed Material Particle Dia. d_{sv} (μm)	U_{mf} (m/s)	U/U_{mf} Range	D/D_t	t_{run}
1,560	479	0.127	1.27–3.85	41.3	90
600	326	0.07	1.32–3.81	41.1	60
600	479	0.127	1.25–3.85	41.1	60
300	286	0.058	1.27–3.85	41.1	45
300	286	0.058	1.27–3.85	20.5	45

Note: Within the U/U_{mf} range stated, 8 different velocities were considered. "t_{run}" refers to the duration of each experiment in minutes.

It was observed that the time spent by the tracers on the bed surface was very short compared with the time spent in the bed (by a factor of at least 10). Also, the time spent by the tracers in the bed was very long compared with the reaction time of an observer watching the taped images (0.2 to 0.3 s). Thus, requirements (a) and (b) were satisfied.

Typically over 300 circulation events were logged (total for the three tracers) for each gas velocity considered. The operating conditions for which the circulation times of the large particles were measured are given in Table 2.

Apart from the correctly scaled conditions investigated in the three beds, two misscaled scenarios were also explored. In one set of experiments, the bed material in the 600-mm bed was replaced with material from the 1,560-mm bed; in another set of experiments, the larger tracers from the 600-mm bed were used in the 300-mm bed.

To compare the results from the large tracer particle experiments, the tracer particle circulation times were distributed into bins in a histogram-style format, and the resulting distributions were then normalized by dividing the number of cycles falling into a given bin range by the total number of cycles over the whole range. (Note that bin widths must be scaled by $\sqrt{m}$ in order to make a meaningful comparison; the bin width times used to present results were 3.22, 2, and 1.41 s in the 1,560-mm, 600-mm, and 300-mm beds, respectively). The time-scale was nondimensionalized by relating time to two scaled-bed properties, the bed diameter, and the particle minimum fluidization velocity

$$t^* = t\left(\frac{U_{mf}}{D}\right) \tag{3}$$

Results and discussion

Figure 3 shows the circulation time distribution comparison for the intermediate gas velocity $U/U_{mf} \approx 2.74$, which was a typical result. The distributions compare well, showing a similar peak dimensionless circulation time in all three fluidized beds for this gas velocity. The size of the peaks are also similar, indicating that the distribution of circulation times for the float tracers within each bed are indeed very similar under these conditions. This sort of agreement in distribution size and shape was typical for the majority of the gas velocities considered.

The only significant departure from the similarity in float tracer circulation behavior occurred at the lowest gas velocity considered, $U/U_{mf} \approx 1.27$. Figure 4 shows this. Float tracers in the smaller two units disappeared at random for much

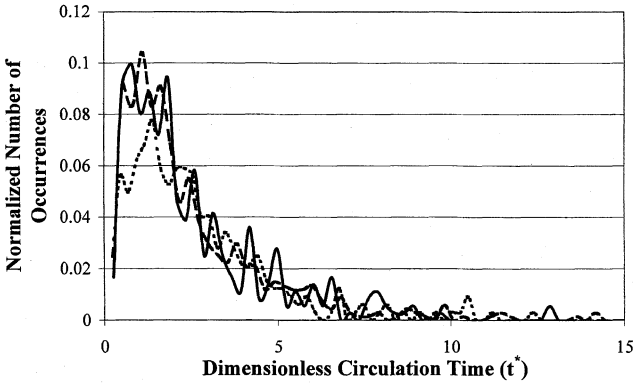

Figure 3. Comparison of the dimensionless circulation time distribution for geometrically scaled float tracers in scaled fluidized beds at $U/U_{mf} \approx 2.75$.

Solids line: $D = 1{,}560$ mm, $U/U_{mf} = 2.76$. Dotted line: $D = 600$ mm, $U/U_{mf} = 2.74$. Dashed line: $D = 300$ mm, $U/U_{mf} = 2.72$.

longer times than their equivalents in the larger bed, which exhibited relatively regular and quite short circulation times. Under these operating conditions, the gas velocity is slightly lower than that required to ensure continuous tuyere operation (Whitehead and Dent, 1967), so there is a possibility of float tracers becoming trapped in stagnant solids for extended periods of time. Occasionally, during a run at low velocity one of the float tracers would disappear permanently; this occurred at least once at all scales and was thought to be due to the tracer becoming lodged in permanently stagnant solids between tuyeres or in the defluidized "corners" between the distributor plate and the vessel wall. The tracer could only be recovered in such cases by stopping the experiment and increasing the gas velocity significantly (to $> 3U_{mf}$) for a short time until all tracers could be seen appearing at the bed surface once again.

At the highest velocity considered ($U/U_{mf} \approx 3.85$), the distributions were still well matched, as Figure 5 shows. The

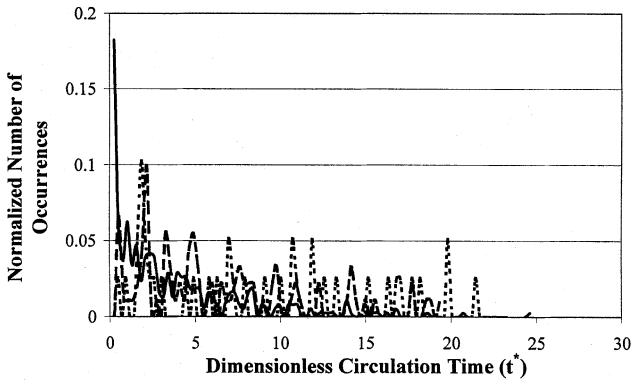

Figure 4. Tracer circulation time distributions for the lowest gas velocities studied ($U/U_{mf} \approx 1.27$).

Solids line: $D = 1{,}560$ mm, $U/U_{mf} = 1.28$. Dotted line: $D = 600$ mm, $U/U_{mf} = 1.32$. Dashed line: $D = 300$ mm, $U/U_{mf} = 1.26$.

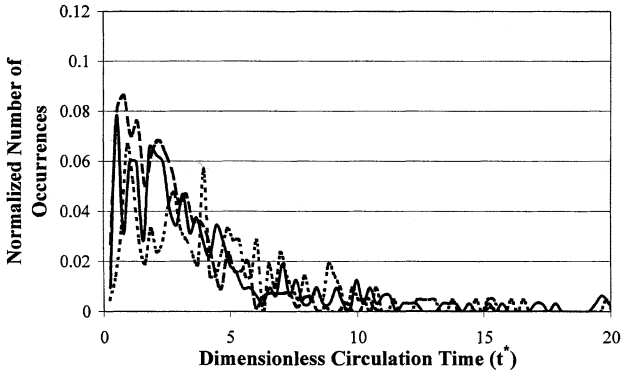

Figure 5. Comparison of the dimensionless circulation time distribution for geometrically scaled float tracers in scaled fluidized beds at $U/U_{mf} \approx 3.85$.

Solids line: $D = 1{,}560$ mm, $U/U_{mf} = 3.84$. Dotted line: $D = 600$ mm, $U/U_{mf} = 3.82$. Dashed line: $D = 300$ mm, $U/U_{mf} = 3.85$.

results for all gas velocities have been summarized in Figure 6, which shows the peak dimensionless circulation time for each bed at each gas velocity.

Examples of the results for the misscaled cases are shown in Figures 7 and 8. The trends were clear at all except the lowest gas velocity (again, likely to be a result of intermittent tuyere operation). The coarser bed material resulted in a broader distribution of circulation times with a longer peak circulation time (Figure 7), and the larger float tracer resulted in a significantly narrower distribution of circulation times with a shorter peak circulation time (Figure 8). The sensitivity of the tracer particle behavior to bed material size and tracer particle diameter demonstrates that the tracer particle circulation time distributions can correctly discriminate between scaled and misscaled conditions. In other words, the tracer behavior is not inherently similar in bubbling beds, but is a scaleable phenomenon.

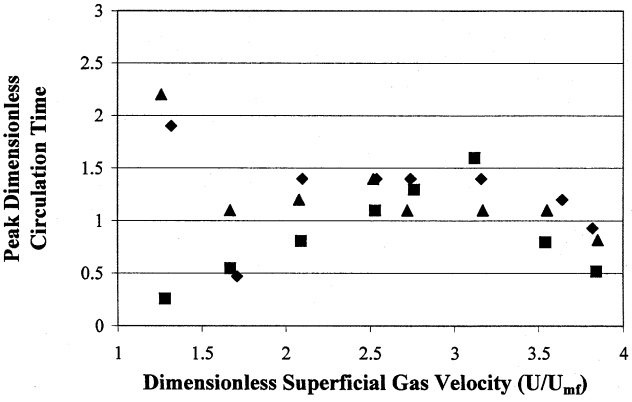

Figure 6. Peak circulation times for float tracers in the correctly scaled fluidized beds at all gas velocities considered.

Squares: $D = 1{,}560$ mm. Diamonds: $D = 600$ mm. Triangles: $D = 300$ mm.

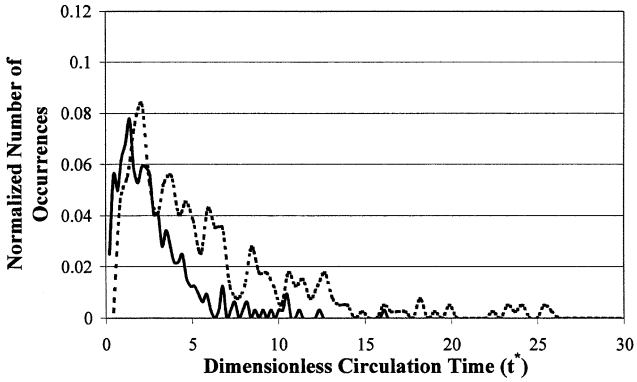

Figure 7. The effect of using a coarser bed material for the same bed diameter, float tracer size, and U/U_{mf} (dimensionless superficial gas velocity).

The original material in the 600-mm bed (solid line, $U_{mf} = 0.070$ m/s) was replaced with material from the 1,560-mm bed (dotted line, $U_{mf} = 0.127$ m/s), with the bed then operated at the same U/U_{mf} (approximately 2.74). The dimensionless circulation time distribution results for the mismatched bed material are compared with those from the original bed material, also fluidized at $U/U_{mf} = 2.74$.

Similarity in Solids Downflow Velocity

Background

There is some evidence to suggest that the solids downflow velocity in a bubbling bed follows the scaling laws. As has already been pointed out (Horio et al., 1986a), a number of bubble-diameter correlations show consistency with the simplified scaling law, and the many experimental verification studies involving bubble-related measurements mentioned earlier tend to support the view that bubble characteristics

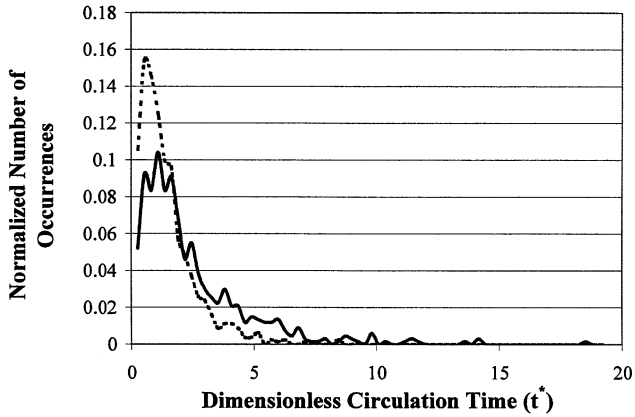

Figure 8. The effect of using a larger float tracer (dotted line, $D/D_t = 20.5$) on the dimensionless circulation time distribution results, compared with the original size used in the similarity experiments (solid line, $D/D_t = 41.1$) for the 300-mm bed fluidized at $U/U_{mf} = 2.72$; in this case only the large particle size has changed, all other operational parameters are identical for both runs.

do scale correctly when using the simplified scaling criteria. The often seen expression for rise velocity of a single bubble (for example, Kunii and Levenspiel, 1991; Clift and Grace, 1985) in which the rise velocity is proportional to the square-root of bubble diameter is also consistent with the scaling law. Now, solids downflow velocity has been related to bubble characteristics by a number of workers. Consider, for example, the correlation of Kunii and Levenspiel (1969), which relates solids downflow velocity to bubble rise velocity by

$$U_{sd} = \frac{\beta_w \epsilon_b U_b}{1 - \epsilon_b - \beta_w \epsilon_b} \tag{4}$$

If the dimensionless ratios β_w (wake fraction) and ϵ_b (visible bubble fraction) are invariant with a scale change made in accordance with the scaling laws, then the solids downflow velocity will scale in proportion with the bubble rise velocity, U_b, and, therefore, be consistent with the scaling law. Note that in their treatment, Kunii and Levenspiel (1969) account for the difference in rise velocity between a single bubble (U_{br}) and multiple bubbles (U_b) by

$$U_b = (U - U_{mf}) + U_{br} \tag{5}$$

Similarly, in the correlation for downwards solids particle velocity as given by Baeyens and Geldart (1986)

$$U_{sd} = \left(\frac{\beta_w + 0.38\beta_d}{1 - \epsilon_b - \epsilon_b(\beta_w + \beta_d)} Y \right) (U - U_{mf}) \tag{6}$$

if the various dimensionless fractions (that is, bubble fraction, wake fraction, and drift fraction and the value Y used to account for the visible bubble fraction being less than predicted by the simple two-phase theory) are all invariant (or close to) with scaling-law scale change, then the first bracketed term of Eq. 6 becomes constant. Thus, solids particle velocity should again scale in direct proportion with excess gas velocity, consistent with the scaling law.

Note that for Eq. 6, it is the value of Y (proportion of excess gas traveling in the form of bubbles) that has the most significant effect. Although Y is found to be a function of the particle diameter (plotted as a function of Archimedes number by Baeyens and Geldart (1986)) for the range of particle diameters considered in this study, it is virtually constant, and the value given by Werther (1978, 1983) of $Y = 0.67$ is appropriate.

The potential agreement of the preceding examples with the simplified scaling law is encouraging. So in addition to the large neutrally buoyant tracer particle study, we attempted to experimentally measure solids downflow velocity in two scaled fluidized beds using a novel application of ECT.

Experimental

The ECT system (UMIST PTL 300 with 12 measurement electrodes) uses the differences in dielectric constant (or permittivity) of the solids and the fluidizing gas to distinguish the emulsion from the bubbles in imaging gas fluidization. It follows (in theory) that the device should be equally capable of resolving two solids with sufficiently different dielectric constants. Readily available materials with different dielectric constants were silica sand and glass ballotini. Initial testing with the ECT unit indicated that the relative difference in the measured capacitance of a packed bed of each material was sufficient to be able to distinguish tracer solids (glass) from bed material (silica sand).

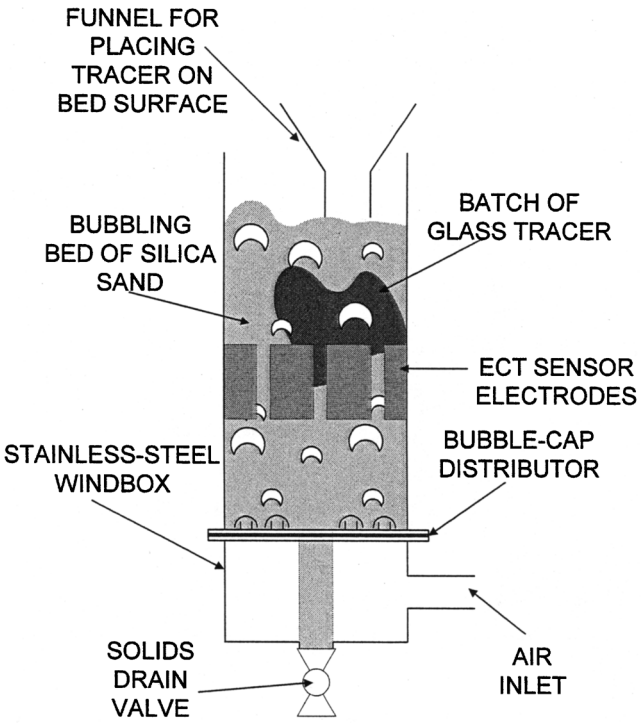

Figure 9. System for measuring solids downflow velocity in the 146-mm and 300-mm dia. beds of silica sand using electrical capacitance tomography and a ballotini tracer.

The approach for inferring a solids downflow velocity was to add a set amount of ballotini tracer to a small region in the radial center of the fluidized-bed surface and look for subsequent changes in the tracer concentration registered at the ECT electrode height. The apparatus is given in Figure 9, with the system being applied to geometrically similar fluidized beds of 146 mm and 300 mm in diameter with aspect ratios of $H_s/D \approx 2{:}1$. Geometrically similar bubble-cap distributors (see Figure 1a) were used. From our observations, the absence of a tuyere in the center of these distributors tends to promote solids downflow at the radial center of the bed. The axial length of the measurement electrodes was 50 mm and 152 mm in the 146-mm and 300-mm beds, respectively; ideally, this corresponds to the axial thickness of the bed that is scanned by the ECT system. Importantly, the axial center of the measurement electrodes was located at very close to the same dimensionless height above the distributor in each bed (150 mm and 300 mm in the 146-mm and 300-mm beds, respectively).

A response profile was generated by averaging the measured concentration values across the ECT measurement cross section every tenth of a second. A 2-s moving average was then applied to the data to smooth out the higher fre-

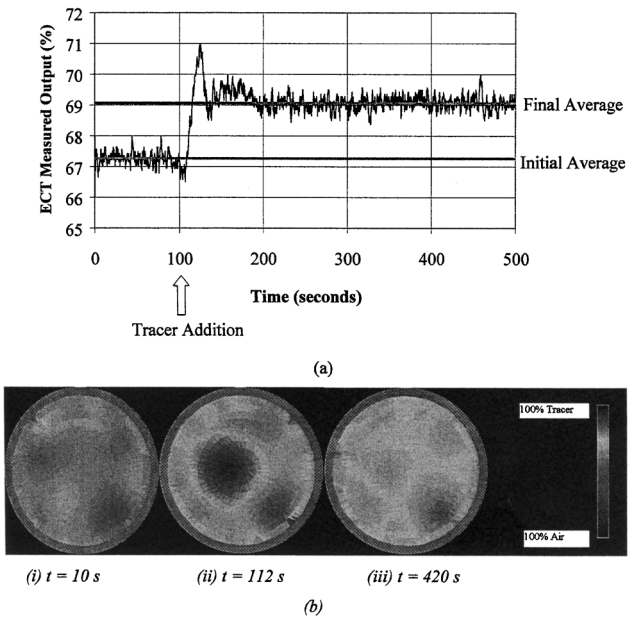

Figure 10. Typical transient tracer response for the addition of ballotini tracer (at $t = 100$ s) to a 146-mm-dia. bubbling bed of sand, measured with the ECT system.

(a) Two-s moving average applied to the spatially averaged ECT system output. One hundred percent on the *y*-axis would correspond to a packed bed of tracer only; 0% corresponds to an empty vessel. (b) Reconstructed images from the ECT data showing (i) the initial bubbling bed of sand, (ii) the clump of descending tracer in the measurement volume, (iii) the bubbling-bed mixture of sand and ballotini after the new steady-state tracer concentration is reached in the ECT measurement volume.

quency "bubble noise" (as the ECT system is sensitive to bubble as well as tracer fluctuations). The resulting transient tracer response profile for a typical run is shown in Figure 10a, with some reconstructed frames of the bed cross section shown for various times in Figure 10b. These results are qualitatively similar to tracer response profiles obtained by previous workers (for example, Avidan and Yerushalmi, 1985), and also agree with the evidence from another study (Fitzgerald et al., 1977) that the tracer solids tend to move downwards in clumps.

On the basis of this observation, it is reasonable to assume that the largest value (the peak) in the transient tracer response profile will correspond to the largest quantity of tracer solids spanning the axial center of the ECT measurement volume. In the current context, the delay from tracer addition to measurement peak can be defined as the time taken for the "average" solids to reach the axial center of the ECT measurement volume as a clump. From this, and a knowledge of the distance between the measurement electrodes and the bed surface, an approximate solids downflow velocity can be calculated. In order to account for the variation in solids mixing behavior from one run to the next [a problem reported by many workers (Fitzgerald et al., 1977; Farrel, 1996; Valenzuela and Glicksman, 1984), multiple runs were performed. Analysis of these runs was then carried out by taking the full set of transient tracer response profiles generated for a given set of conditions, removing any offset associated with the initial measured concentration for each run, and averaging the whole set of profiles, to generate one "average" tracer response profile for a given set of conditions. This average profile, usually constructed using results from 14 individual experiments, was then used in subsequent calculations of solids downflow velocity.

Table 3. Operating Conditions and Tracer/Bed Material Combinations for the Solids Downflow Velocity Similarity Experiments

	Bed Dia. D (mm)	Bed Material d_{sv} (μm)	Tracer d_{sv} (μm)	U_{mfBM} (m/s)	U_{mfT} (m/s)	U (m/s)	U/U_{mfBM}
Pair 1	146	230	269	0.039	0.048	0.056	1.44
	300	286	347	0.058	0.079	0.084	1.45
Pair 2	146	304	269	0.046	0.048	0.066	1.43
	300	326	347	0.070	0.079	0.100	1.43
Pair 3	146	344	369	0.085	0.085	0.122	1.44
	300	388	369	0.125	0.085	0.180	1.44

Note: 14 runs were carried out in each bed for each condition listed. Subscripts BM and T refer to bed material and tracer, respectively.

In the similarity comparison, three "pairs" of scaled beds were considered at the two scales, with tracer always added at $t = 100$ s. The bed materials and superficial gas velocities were selected in accordance with the simplified scaling criteria; Group B materials were used in all cases, although tracer and bed material had somewhat different sphericities ($\Phi = 1$ and 0.86, respectively). Particle-size distributions for all bed and tracer materials have been presented in Sanderson, (2003). The conditions for which the solids downflow velocity was measured are given in Table 3. Settled bed heights were 295 mm and 590 mm for the 146-mm and 300-mm beds, respectively; scaled tracer quantities of 250 mL and 2,000 mL were added to each bed per run. Although the minimum fluidization velocities of the tracers and bed materials should be identical, this was not possible given the tracer materials available, so the ratio of tracer U_{mf} to bed material U_{mf} was kept approximately the same.

The influence of tracer/bed material size mismatch on solids downflow velocity was explored in separate experiments (Sanderson, 2003); generally, $U_{mfT} > U_{mfBM}$ led to a faster downflow velocity, and $U_{mfT} < U_{mfBM}$ led to a slower downflow velocity and segregation in some cases. The effect of the tracer addition on the overall bed hydrodynamics (given the differences in U_{mf}, as well as particle shape and density) were minimized by keeping the overall concentration of tracer in the bed small during the experiments and replacing the entire bed with fresh bed material frequently.

Results and discussion

Averaged transient tracer response profiles for the solids downflow velocity are shown in Figures 11 and 12 for the 146-mm and 300-mm beds, respectively. (The profiles correspond to the first two listings of Table 3.) The profiles have a qualitatively similar appearance and the time-to-peak in the larger scale system is somewhat longer than that for the smaller system, as expected for scaled behavior (from the scaling law, the time-scale is expected to increase by a factor of $\sqrt{m}$).

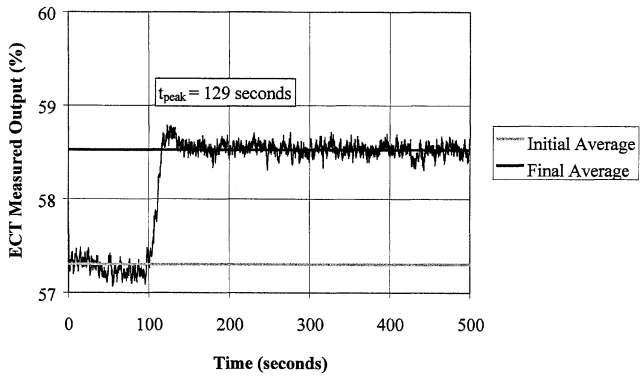

Figure 11. Averaged tracer response profile for the solids downflow velocity similarity experiment in 146-mm bed (U_{mfBM} = 0.039m/s).

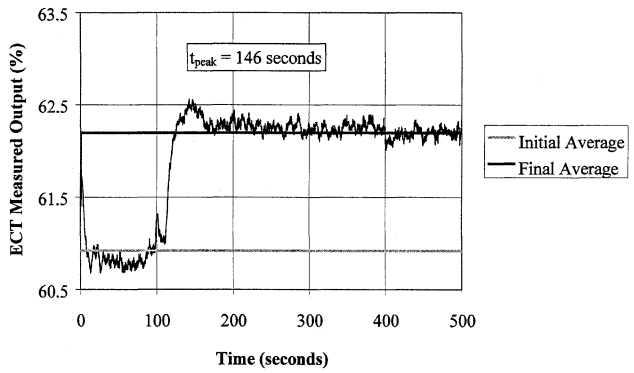

Figure 12. Averaged tracer response profile for the solids downflow velocity similarity experiment in 300-mm bed (U_{mfBM} = 0.058 m/s).

The solids downflow velocity was calculated from the following equation

$$U_{sd} = \frac{\Delta h}{\Delta t} = \frac{H_s - H_e}{t_{\text{peak}} - t_{\text{added}}} \tag{6}$$

where the settled bed height H_s was used (somewhat arbitrarily) to account for the fact that the tracer deposited on the bed surface does not sit "on" the surface, but sinks into it immediately, presenting an even bed surface at $t = 100$ s. Results for solids downflow velocity are shown in Table 4.

Also included are solids downflow velocities estimated using the correlations of Kunii and Levenspiel (1969) and Baeyens and Geldart (1986). These were calculated using appropriate estimates for the various "fractions," based on the recommendations accompanying each of the correlations. (There is certainly some flexibility in the choice of these values, and different assumptions for β_w, β_d, ϵ_b, and Y will affect the calculated result, of course. Ultimately, however, the effect on U_{sd} is small for all parameters except Y, and this is likely to be constant for the conditions investigated (Baeyens and Geldart, 1986).) Given the differences in the approaches, it is expected that the Baeyens and Geldart correlation will result in a higher solids downflow, since they are assuming a greater proportion of each rising bubble is capable of solids transport.

As can be seen from Table 4, the agreement between the measured downflow velocities and those predicted by the correlations is approximate. According to the simplified scaling laws, for a length scale change of m, the characteristic velocity should scale by $\sqrt{m}$, and this should apply to the solids downflow velocities. For the bed diameters here, $\sqrt{m} = 1.43$ and the ratios of the experimentally determined U_{sd} for the first two cases are 1.26 and 1.64, respectively, so the agreement is qualitative at best. The correlation results scale a little better (and would scale perfectly if the "fractions" estimated were exactly the same). In the last instance listed (300-mm bed), no result could be obtained because there was no peak in the response profile. Unfortunately, in this case the tracer material was significantly smaller than the bed material and segregation effects dominated.

The precision of the solids downflow velocity results was limited because the ECT system responds to both bubbles and tracer; the bubbles add an undesirable layer of "noise" to the tracer response profiles. Based on our observations, the use of a tracer with a higher dielectric constant would significantly improve the success of this experimental technique, as it would provide a stronger peak in the response profile. Also, better matching of the particle and tracer properties may well improve the results, as we have had to assume that particle size, sphericity, and minor density differences between tracer and bed material do not influence the results. (If the solids mixing behavior is dominated by bubble activity and the quantity of tracer added is insufficient to alter bubble characteristics, then this assumption may be reasonable.)

Conclusions

Although it is some time since the hydrodynamic similarity criteria for bubbling beds were first proposed, there has been limited experimental evaluation of these criteria using solids

Table 4. Results for Solids Downflow Velocity in Scaled Beds, Compared with Predictions of Eq. 4* and Eq. 6**

	Bed Dia. D (mm)	U_{sd} (*expt*) (mm/s)	U_{sd}* (mm/s)	U_{sd}** (mm/s)	Correlation Parameters ε_b, β_w, β_d, Y
Pair 1	146	5.0	2.5	5.0	0.03, 0.26, 0.42, 0.67
	300	6.3	3.8	7.4	0.03, 0.25, 0.4, 0.67
Pair 2	146	3.9	2.9	6.0	0.04, 0.26, 0.42, 0.67
	300	6.4	4.4	7.8	0.04, 0.23, 0.25, 0.67
Pair 3	146	7.3	5.6	10.0	0.06, 0.23, 0.35, 0.67
	300	N/A	8.7	14.6	0.05, 0.23, 0.35, 0.67

*Kunii and Levenspiel (1969).
**Baeyens and Geldart (1986).

motion studies. Evidence from various previous studies and literature correlations tends to suggest that large, neutrally buoyant particle motion and solids downflow velocity should exhibit scaled behavior, and in this work we have tested the simplified scaling laws by comparing the motion of large tracer particles in one set of experiments and solids downflow velocity in another.

We found that our experimental approach to large-particle circulation monitoring was a simple and effective method for solids motion comparisons. The circulation of the large particles within the correctly scaled bubbling beds was consistent with the scaling law across a wide range of bed diameters; this has useful consequences for some fluidized-bed applications (such as combustors). The tracer particle circulation rate was sensitive to both tracer particle size and bed material selection, mismatching either of these resulted in poor agreement. However, altering the tracer density within a limited range (1,310 to 1,410 kg/m^3) had no effect on the circulation time distributions, implying that some flexibility is allowable in selecting the relative density of the large tracer and the bed emulsion (not to be confused with the solids-to-gas density ratio requirements of the similarity criteria that have been matched throughout this study).

Our results for solids downflow velocity in the scaled beds showed qualitative agreement with the simplified scaling law and literature correlations. In these initial trials of a new measurement technique for solids mixing, the precision of the results was limited because the ECT system responds to both bubbles and tracer; the bubbles add an undesirable layer of "noise" to the tracer response profiles. We also found that matching of the tracer and bed material fluidization properties was somewhat difficult. Based on our observations, the use of a tracer with a higher dielectric constant, and a better matching of the particle and tracer properties would significantly improve the success of this experimental technique. The application of this technique to "bubbleless" fluidization may also be a worthwhile area of future work.

Acknowledgments

This work received financial and other support from the Cooperative Research Centre for Clean Power from Lignite through the Australian Government's Cooperative Research Centres Scheme. The authors are also grateful for the financial support of the Strategic Monash University Research Fund. Initial ECT mixing experiments were carried out with the help of high-school students James Masters and Caryn Eberius through the 1999 CSIRO Student Research Scheme. The authors wish to acknowledge the suggestions and advice of Dr. K. S. Lim regarding some aspects of the experimental work, and Dr. R. J. van Wegen for assisting with data-analysis software.

Notation

d_{sv} = Sauter mean diameter $= 1/\Sigma \frac{V_i}{d_i}$
d_i = mean class diameter, μm
D = bed diameter, mm, except Eq. 3; m
D_t = large tracer particle diameter, mm
H_s = settled bed height, mm
H_e = ECT sensor electrode height, mm
L = characteristic length, m
m = characteristic length ratio ($m = D_2/D_1$)
t_{peak} = time to tracer concentration peak, s
t_{added} = time tracer material was added, s
t = time, s
t^* = dimensionless time
t_{run} = large tracer particle monitoring time, s
U = superficial gas velocity, m/s
U_B = average measured bubble rise velocity from Lim and Agarwal (1994), m/s
U_b = rise velocity of bubbles in a swarm, from Kunii and Levenspiel (1969), m/s
U_{br} = rise velocity of a single isolated bubble, from Kunii and Levenspiel (1969), m/s
u_{mf} = minimum fluidization velocity, m/s
U_{sd} = solids downflow velocity, mm/s
V_i = relative volume of the ith sample
Y = proportion of excess gas traveling in the form of bubbles

Greek letters

β_d = drift fraction
β_w = wake fraction
ϵ_b = visible bubble fraction
Φ = particle sphericity
$\rho_{bed(mf)}$ = bed density at minimum fluidization, kg/m^3
ρ_f = gas density, kg/m^3
ρ_s = solid density, kg/m^3
ρ_t = density of large tracer particle, kg/m^3

Subscripts

1,2 = denotes bed scales
BM = bed material
T = tracer

Literature Cited

Agarwal, P. K., and R. D. LaNauze, "Transfer Processes Local to the Coal Particle: A Review of Drying, Devolatilization and Mass Transfer in Fluidized Bed Combustion," *Chem. Eng. Res. Des.*, **67**, 457 (1989).

Almstedt, A. E., and V. Zakkay, "An Investigation of Fluidized Bed Scaling—Capacitance Probe Measurements in a Pressurized Fluidized-Bed Combustor and a Cold Model Bed," *Chem. Eng. Sci.*, **45**, 1071 (1990).

Avidan, A., and J. Yerushalmi, "Solids Mixing in an Expanded Top Fluid Bed," *AIChE J.*, **31**(5), 835 (1985).

Baeyens, J., and D. Geldart, "Solids Mixing," *Gas Fluidization Technol.*, D. Geldart, ed., Wiley, p. 107 (1986).

Bellgardt, D., and J. Werther, "A Novel Method for the Investigation of Particle Mixing in Gas-Solid Systems," *Powder Technol.*, **48**, 173 (1986).

Clift, R., and J. R. Grace, *Fluidization*, 2nd ed., J. F. Davidson, ed., Academic Press, New York, p. 73 (1985).

Farrel, P. A., "Hydrodynamic Scaling and Solids Mixing in Pressurised Bubbling Fluidized Bed Combustors," PhD Diss., Mechanical Engineering Dept., Massachusetts Institute of Technology, Cambridge (1996).

Farrel, P. A., M. R. Hyre, and L. R. Glicksman, "Importance of the Solid to Gas Density Ratio for Scaling Fluidized Bed Hydrodynamics," *Proc. Fluidization IX*, Engineering Foundation, New York, p. 85 (1998).

Fitzgerald, T. J., and S. D. Crane, "Cold Fluidized Bed Modelling," *Proc. Int. Conf. Fluidized Bed Combustion*, Vol. III, Technical Sessions, p. 815 (1980).

Fitzgerald, T., N. Catipovic, and G. Jovanovic, "Solid Tracer Studies in a Tube-Filled Fluidized Bed," *Proc. Int. Conf. on Fluidized Bed Combustion*, Vol. III, Washington, D.C., p. 135 (1977).

Fitzgerald, T., D. Bushnell, S. Crane, and Y.-C. Hsieh, "Testing of Cold Scaled Bed Modelling for Fluidized Bed Combustors," *Powder Technol.*, **38**, 107 (1984).

Glicksman, L. R., "Scaling Relationships for Fluidized Beds," *Chem. Eng. Sci.*, **39**, 1373 (1984).

Glicksman, L. R., "Scaling Relationships for Fluidized Beds," *Chem. Eng. Sci.*, **43**(6), 1419 (1988).
Glicksman, L. R., M. Hyre, and K. Woloshun, "Simplified Scaling Relationships for Fluidized Beds," *Powder Technol.*, **77**, 177 (1993).
Hesketh, R. P., and J. F. Davidson, "The Effect of Volatiles on the Combustion of Char in a Fluidized Bed," *Chem. Eng. Sci.*, **46**, 3101 (1991).
Horio, M., A. Nonaka, Y. Sawa, and I. Muchi, "A New Similarity Rule for Fluidized-Bed Scale-Up," *AIChE J.*, **32**, 1466 (1986).
Horio, M., M. Takada, M. Ishida, and N. Tanaka, "The Similarity Rule of Fluidization and Its Application to Solid Mixing and Circulation Control," *Proc. Fluidization V*, Engineering Foundation, New York, 151 (1986).
Kunii, D., and O. Levenspiel, *Fluidization Engineering*, Wiley, New York, p. 155 (1969).
Kunii, D., and O. Levenspiel, *Fluidization Engineering*, Butterworth-Heinmann, Boston, p. 147 (1991).
Leu, L. P., and C. W. Lan, "Scale-up of Gas-Solid Bubbling Fluidized Beds—Verification and Comment on Scale Up Rules," *J. Chin. Inst. Chem. Eng.*, **23**(1), 35 (1992).
Lim, K. S., and P. K. Agarwal, "Circulatory Motion of a Large and Lighter Sphere in a Bubbling Fluidized Bed of Smaller and Heavier Particles," *Chem. Eng. Sci.*, **49**(3), 421 (1994).
Merry, J. M. D., and J. F. Davidson, "'Gulf-Stream' Circulation in Shallow Fluidized Beds," *Trans. Inst. Chem. Eng.*, **51**, 361 (1973).
Newby, R. A., and D. L. Keairns, "Test of the Scaling Relationships for Fluid-Bed Dynamics," *Proc. Fluidization V*, Engineering Foundation, New York, p. 31 (1986).
Nguyen, T. H., and J. R. Grace, "Forces on Objects Immersed in Fluidized Beds," *Powder Technol.*, **19**, 255 (1978).
Nicastro, M. T., and L. R. Glicksman, "Experimental Verification of Scaling Relationships for Fluidized Bed," *Chem. Eng. Sci.*, **39**, 1381 (1984).
Nienow, A. W., P. N. Rowe, and T. Chiba, "Mixing and Segregation of a Small Proportion of Large Particles in Gas Fluidized Beds of Considerably Smaller Ones," *AIChE Symp. Ser.*, **176**, Vol. 74, 45 (1978).
Prins, W., R. Siemons, W. P. M. van Swaaij, and M. Radovanovic, "Devolatilization and Ignition of Coal Particles in a Two-Dimensional Bed," *Combust. Flame*, **75**, 57 (1989).
Rios, G. M., K. D. Tran, and H. Masson, "Free Object Motion in a Gas Fluidized Bed," *Chem. Eng. Commun.*, **47**, 247 (1986).
Roy, R., and J. F. Davidson, "Similarity Between Gas-Fluidized Beds at Elevated Temperature and Pressure," *Proc. Fluidization VI*, Engineering Foundation, New York, p. 293 (1989).
Sanderson, P. J., PhD Diss., Dept. of Chemical Engineering, Monash University, Australia (2003).
Sanderson, P. J., M. J. Rhodes, and P. R. Sanderson, "Testing the Simplified Scaling Laws for Bubbling Fluidized Beds," *Proc. Fluidization X*, Engineering Foundation, New York, p. 381 (2001).
Stein, M., J. Seville, D. Parker, and D. Allen, "Scale-Up of Particle Motion in Fluidized Beds Using Positron Emission Particle Tracking," *Proc. Fluidization IX*, Engineering Foundation, New York, p. 77 (1998).
Valenzuela, J. A., and L. R. Glicksman, "An Experimental Study of Solids Mixing in a Freely Bubbling Two-Dimensional Fluidized Bed," *Powder Technol.*, **38**, 63 (1984).
Werther, J., *Ger. Chem. Eng.*, **1**, 243 (1978).
Werther, J., *Fluidization IV*, Japan (1983).
Whitehead, A. B., and D. C. Dent, "Behaviour of Multiple Tuyere Assemblies in Large Fluidized Beds," *Proc. Int. Symp. on Fluidization*, A. A. H. Drinkenberg, ed., Eindhoven, Netherlands Univ. Press, Amsterdam, p. 802 (1967).

Manuscript received Nov. 27, 2001, revision received Aug. 6, 2002, and final revision received Feb. 18, 2003.